AMERICAN SOCIETY of
GENE & CELL
THERAPY

Antisense Oligonucleotide Inhibition of MicroRNA-494 Halts Atherosclerotic Plaque Progression and Promotes Plaque Stabilization

Eva van Ingen,[1,2] Amanda C. Foks,[3] Mara J. Kröner,[3] Johan Kuiper,[3] Paul H.A. Quax,[1,2] Ilze Bot,[3]
and Anne Yaël Nossent[1,2,4,5]

[1]Department of Surgery, Leiden University Medical Center, 2300 RC, Leiden, the Netherlands; [2]Einthoven Laboratory for Experimental Vascular Medicine, Leiden University Medical Center, 2300 RC, Leiden, the Netherlands; [3]Division BioTherapeutics, LACDR, Leiden University, 2333 CC, Leiden, the Netherlands; [4]Department of Internal Medicine II, Medical University of Vienna, 1090 Vienna, Austria; [5]Department of Laboratory Medicine, Medical University of Vienna, 1090 Vienna, Austria

We have previously shown that third-generation antisense (3GA) inhibition of 14q32 microRNA (miRNA)-494 reduced early development of atherosclerosis. However, patients at risk of atherosclerotic complications generally present with advanced and unstable lesions. Here, we administered 3GAs against 14q32 miRNA-494 (3GA-494), miRNA-329 (3GA-329), or a control (3GA-ctrl) to mice with advanced atherosclerosis. Atherosclerotic plaque formation in $LDLr^{-/-}$ mice was induced by a 10-week high-fat diet and simultaneous carotid artery collar placement. Parallel to 3GA-treatment, hyperlipidemia was normalized by a diet switch to regular chow for an additional 5 weeks. We show that, even though plasma cholesterol levels were normalized after diet switch, carotid artery plaque progression continued in 3GA-ctrl mice. However, treatment with 3GA-494 and, in part, 3GA-329 halted plaque progression. Furthermore, in the aortic root, intra-plaque collagen content was increased in 3GA-494 mice, accompanied by a reduction in the intra-plaque macrophage content. Pro-atherogenic cells in the circulation, including inflammatory Ly6C^hi monocytes, neutrophils, and blood platelets, were decreased upon miRNA-329 and miRNA-494 inhibition. Taken together, treatment with 3GA-494, and in part with 3GA-329, halts atherosclerotic plaque progression and promotes stabilization of advanced lesions, which is highly relevant for human atherosclerosis.

INTRODUCTION

Atherosclerosis is a chronic inflammatory disease characterized by progressive plaque buildup in the arterial wall. Most plaques that develop during one's life remain clinically silent. However, lesion progression and disruption of a vulnerable plaque may result in a cardiovascular event, such as an ischemic stroke or myocardial infarction.[1] Surgical interventions to prevent, for example, ischemic stroke are carotid endarterectomy or stenting, but due to the perioperative risks, these are only performed when a plaque causes a stenosis of the carotid artery of more than 70% or when the plaque is symptomatic, i.e., causing transient ischemic attacks (TIAs).[2]

An established therapeutic strategy is plasma lipid lowering by statins. Lipid-lowering strategies have been shown to contribute to increased plaque stability and reduce the risk of (recurrent) cardiovascular events, including myocardial infarction.[3–5] Independent of lipid lowering, targeting inflammation is also important in reducing the incidence of recurrent cardiovascular events, as was demonstrated in the canakinumab anti-inflammatory thrombosis outcome study (CANTOS) trial.[6] Although current therapeutic strategies contribute to reducing the risk of recurrent cardiovascular events, a clinical need remains for novel noninvasive therapies targeting multiple aspects of atherosclerosis and improving clinical outcome. Therapeutic strategies increasing stabilization of vulnerable plaques, alone or complemented by existing lipid-lowering treatments, would be of great clinical value in reducing the risk of thrombotic events in the carotid, coronary, and peripheral arteries.

MicroRNAs (miRNAs) are post-transcriptional negative regulators of gene expression. Because of their ability to fine-tune expression of multiple target genes, miRNAs are promising drug targets for complex diseases, including atherosclerosis.[7] Several studies have focused on the therapeutic potential of miRNA-modulation in atherosclerosis. For example, the miRNA-33 family, including miRNA-33a and miRNA-33b, regulates cholesterol metabolism by targeting cholesterol transporter ABCA1. Inhibition of miRNA-33 resulted in decreased very low-density lipoprotein (VLDL), whereas high-density lipoprotein (HDL) was increased in the plasma.[8–10] More recently, it was shown that miRNA-33 inhibition also promotes cholesterol efflux from arterial macrophages and thereby directly regulates atherosclerotic plaque formation.[11] Inflammation in atherosclerosis was reduced via miRNA-155 inhibition. miRNA-155 is predominantly expressed in pro-inflammatory macrophages. Inhibition
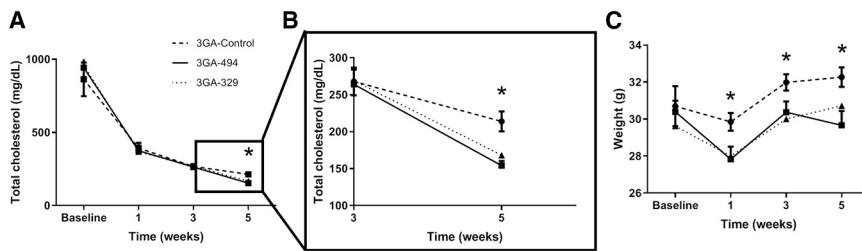
Figure 1. Total Cholesterol Levels and Bodyweight Levels of *LDLr*^{−/−} Mice Treated with 3GA-ctrl, 3GA-494, or 3GA-329

Mice received 3GA treatment immediately after (baseline) and 2 and 4 weeks after diet replacement from high-fat high cholesterol to regular chow. All mice were sacrificed at week 5. (A) Total cholesterol (TC) levels in mg/dL measured in the serum of 3GA-ctrl-, 3GA-494-, and 3GA-329-treated mice, quantified by using enzymatic procedures, at baseline and up to 5 weeks after diet replacement. (B) Zoomed-in graph of TC at weeks 3 and 5. (C) Bodyweight levels in g after diet replacement. A two-tailed Student's t test was performed to compare single treatment to the 3GA-ctrl group at each time point. *p < 0.05 compared to 3GA-ctrl. 3GA-ctrl (N = 10), 3GA-494 (N = 10), and 3GA-329 (N = 8). Data are represented as mean ± SEM.

of miRNA-155 resulted in smaller atherosclerotic lesions containing fewer lipid-laden macrophages via increasing expression of its target BCL6, which attenuates pro-inflammatory nuclear factor κB (NF-κB) signaling.[12] Furthermore, plaque stability was shown to increase upon overexpressing miRNA-210. miRNA-210 inhibits adenomatous polyposis coli (APC) expression in smooth muscle cells (SMCs) and thereby enhances intra-plaque SMC survival and, thus, intra-plaque collagen synthesis.[13] However, as one miRNA can have multiple target genes, single miRNAs also have the potential to target all aspects of atherosclerosis at once. For example, inhibition of miRNAs transcribed from the 14q32 cluster (12F1 in mice) targeted multiple aspects in atherosclerosis, including lipid hemostasis, inflammation, and concomitant plaque development, as we have shown previously.[14]

The 14q32 cluster is the largest known miRNA gene cluster in humans and contains more than 50 miRNA genes. We have evaluated the therapeutic inhibition of 14q32 miRNAs in different vascular remodeling processes.[14–17] In two different murine models of vascular remodeling, one for intimal hyperplasia and one for accelerated atherosclerosis, we showed that inhibition of 14q32 miRNAs reduced initial lesion development, increased plaque stability, and decreased plasma cholesterol levels.[14,16] Importantly, inhibition of 14q32 miRNAs reduced macrophage influx in the intima in the intimal hyperplasia model.[16] These studies, however, focused on the effects of 14q32 miRNA inhibition in initial lesion development,[14] where most patients present in the clinic with advanced, symptomatic atherosclerotic lesions.

In the current study, we therefore aimed to investigate the effects of 14q32 miRNA inhibition on advanced lesions. We used third-generation antisense (3GA) to inhibit two different 14q32 miRNAs, miRNA-494 and miRNA-329. Parallel to 3GA treatment, we included a diet switch from high-fat high-cholesterol to regular chow to normalize hyperlipidemia, in order to closely mimic routine lipid-lowering treatment.

First, we show that inhibition of 14q32 miRNAs, particularly miRNA-494, halted atherosclerotic plaque progression and increased plaque stability in mice with advanced atherosclerotic lesions. Second, we show that plasma cholesterol levels show a modest but further reduc-

tion after miRNA-494 and miRNA-329 inhibition. Third, we show that pro-atherogenic cells in the circulation, including inflammatory Ly6C^{hi} monocytes, neutrophils, and platelets, were decreased upon miRNA-329 and miRNA-494 inhibition, which is highly relevant in further reducing the risk of atherosclerotic complications.

RESULTS

3GA-494 and 3GA-329 Treatment Reduces Plasma Cholesterol Levels and Body Weight

The timeline of the study is shown in Figure S1. Plasma cholesterol levels showed a clear decrease in all groups after diet replacement (Figure 1A). Both 3GA-494- and -329-treated groups showed a further reduction in total plasma cholesterol levels compared to the 3GA-control (3GA-ctrl) 5 weeks after diet switch (3GA-494, 155 ± 6 mg/dL; 3GA-329, 168 ± 11 mg/dL; versus 3GA-ctrl, 214 ± 13 mg/dL, p < 0.05; Figure 1B). Similar to as shown previously,[18] body weight did not significantly differ after diet switch in the 3GA-ctrl group as compared to baseline but showed a reduction in 3GA-494- or 3GA-329-treated mice compared to 3GA-ctrl (Figure 1C). Subsequently, all groups increased in body weight during the remainder of the study, independent of the treatment, but body weight levels of 3GA-494- and 3GA-329-treated mice remained decreased compared to 3GA-ctrl. The size of the spleen was increased in all of the 3GA-494-treated mice and in half of the 3GA-329-treated mice, as is further described below. All other organs appeared normal, and mice did not show any pathological changes.

3GA-494 Treatment Halts Plaque Progression in the Carotid Artery

In the carotid arteries, miRNA-494 and miRNA-329 expression were inhibited in both 3GA-494 and 3GA-329, respectively, compared to 3GA-ctrl (Figure 2A). miRNA-494 and miRNA-329 target gene expression levels (miRNA-494—IL33, TIMP3, and TLR4; miRNA-329—VEGFA, Mef2A, and TLR4), however, were not significantly different compared to the control 1 week after final 3GA injections (Figures S2A and S2B). 3GA-ctrl-treated mice showed increased carotid artery average plaque size compared to baseline, indicating continued atherogenesis, even after lowering plasma cholesterol levels by diet replacement (baseline, 18 ± 4 × 10^{3} μm[2], versus 3GA-ctrl, 32 ± 10 × 10^{3} μm[2]; Figures 2B and 2D). At the site of maximal stenosis, plaque size was increased in 3GA-ctrl compared
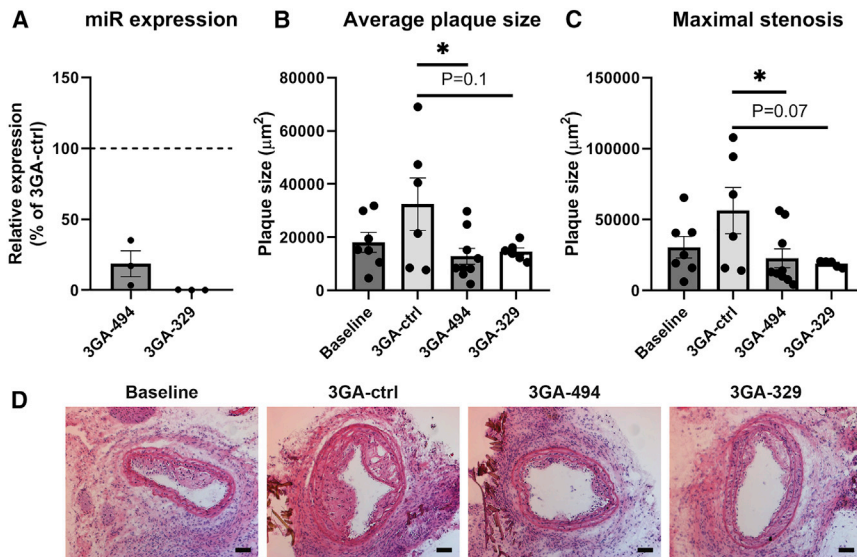
Figure 2. Inhibition of miRNA-494 and miRNA-329 in Atherosclerotic Lesions in the Carotid Artery

(A) Levels of miRNA-494 (N = 3) and miRNA-329 (N = 3) in carotid arteries of $LDLr^{-/-}$ mice 1 week after the final injection of 3GA-494 and 3GA-329, respectively, normalized to miRNA-494 and miRNA-329 expression in mice treated with 3GA-ctrl (100%; N = 3). miRNA-191 was used as a reference gene. (B) Average plaque size (calculated as the size average of plaque sections taken 100 μm apart) in the carotid arteries of baseline (N = 7), 3GA-ctrl (N = 6), 3GA-494 (N = 8), and 3GA-329 mice (N = 6) and (C) plaque size at the site of maximal stenosis in μm² in the carotid arteries of baseline (N = 7), 3GA-ctrl (N = 6), 3GA-494 (N = 8), and 3GA-329 mice (N = 6). (D) Representative images of all groups. Scale bar, 100 μm. A two-tailed Student's t test was performed to compare single treatment to the 3GA-ctrl group. A Grubbs' test was used to identify significant outliers (α < 0.05). *p < 0.05 compared to 3GA-ctrl. Data are represented as mean ± SEM.

to baseline (baseline, $30 \pm 8 \times 10^3$ μm², versus 3GA-ctrl, $56 \pm 16 \times 10^3$ μm²; Figure 2C). In 3GA-494 mice, carotid artery plaque size was significantly decreased compared to 3GA-ctrl. In fact, 3GA-494 mice had similar plaque sizes to baseline mice in both average plaque sizes (baseline, $18 \pm 4 \times 10^3$ μm²; 3GA-ctrl, $32 \pm 10 \times 10^3$ μm², versus 3GA-494, $13 \pm 3 \times 10^3$ μm², p < 0.05; Figures 2B and 2D) and at the site of maximal stenosis (baseline, $30 \pm 8 \times 10^3$ μm²; 3GA-ctrl, $56 \pm 16 \times 10^3$ μm²; versus 3GA-494, $23 \pm 7 \times 10^3$ μm², p < 0.05; Figure 2C). 3GA-329-treated mice showed a trend toward a smaller average plaque size and at the site of maximal stenosis (average, 3GA-329, $15 \pm 1 \times 10^3$ μm², p = 0.09; maximal stenosis, 3GA-329, $21 \pm 3 \times 10^3$ μm², p = 0.1; Figures 2B–2D). Due to the small size, most plaques showed a fatty streak phenotype rather than an advanced atherosclerotic plaque phenotype. Advanced atherosclerotic plaque features, such as a fibrous cap and necrotic core, were lacking in most plaques, and therefore, we were unable to quantify and compare this among the groups.

Inhibition of miRNA-494 Increases Plaque Stability in Advanced Plaques

In the aortic root, plaque size and necrotic core size did not differ between groups (Figures 3A and 3B). Other markers for plaque stability, however, were increased after miRNA-494 and, in part, miRNA-329 inhibition (Figures 3C–3E). Intra-plaque collagen content was strongly increased in 3GA-494 mice compared to the control (3GA-ctrl, 37% ± 3%, versus 3GA-494 55% ± 3%, p < 0.0005; Figure 3C). Treatment with 3GA-329 resulted in four mice in increased collagen content, whereas the other four showed similar collagen content as baseline mice (baseline, 15% ± 2%, versus 3GA-329, 34% ± 9%; Figure 3C). SMCs are the main source of collagen synthesis in atherosclerotic plaques, but the SMC content was similar in all groups (baseline, 12% ± 1%; 3GA-ctrl, 14% ± 1%; 3GA-494, 11% ± 1%; 3GA-329, 13% ± 1%; Figure 3D). Relative intra-plaque macrophage area was reduced upon diet switch from

diet with high-fat high-cholesterol to regular chow (baseline, 22% ± 2%, versus 3GA-ctrl, 17% ± 2%; Figure 3E). In 3GA-494 mice, a further reduction in intra-plaque macrophage content was shown (3GA-ctrl, 17% ± 2%, versus 3GA-494, 12% ± 1%, p < 0.05; Figure 3E), which is another marker of increased plaque stability. For the 3GA-329 treated mice, the relative macrophage area remained similar to control levels (3GA-329, 17% ± 2%; Figure 3E). Numbers of intra-plaque neutrophils were very small and not different among the groups (data not shown). Plaque necrotic core sizes were not significantly different between groups as well (Figure 3E).

Blood, Spleen, and Lymph Node Analyses of $LDLr^{-/-}$ Mice Treated with 3GA-494, 3GA-329, or 3GA-ctrl

Blood analysis by Sysmex and flow cytometry revealed altered numbers of circulating cells upon 3GA-494 and 3GA-329 treatment compared to 3GA-ctrl (Figure 4 and Figure S3). White blood cells (WBCs) remained similar after miRNA-494 inhibition but were decreased after miRNA-329 inhibition (Figure 4A). Myeloid cells, as defined by CD11b⁺ and CD11c⁺CD11b⁺, were elevated in 3GA-494 mice, whereas CD11b⁺ cells were decreased in 3GA-329 mice (Figures S3A and S3B). More specifically, we observed that neutrophils (Ly6C⁺Ly6Gⁱⁿᵗ), which are part of the myeloid compartment of WBCs, were decreased after miRNA-494 and miRNA-329 inhibition (Figures 4B and 4C). The total monocyte count, also part of the myeloid compartment of WBCs, was not significantly altered, although we did observe differences in the pro-inflammatory subset (Ly6C⁺Ly6G⁻) quantified by fluorescence-activated cell sorting (FACS) analysis (Figures 4D and 4E).

Although total amounts of lymphocytes were similar, CD19⁺ B cells were reduced in 3GA-494 mice, and CD4⁺ and CD8⁺ T cells were slightly increased in 3GA-329 mice (Figure 4F and Figures S3C–S3E). Furthermore, miRNA-494 inhibition decreased red blood cell
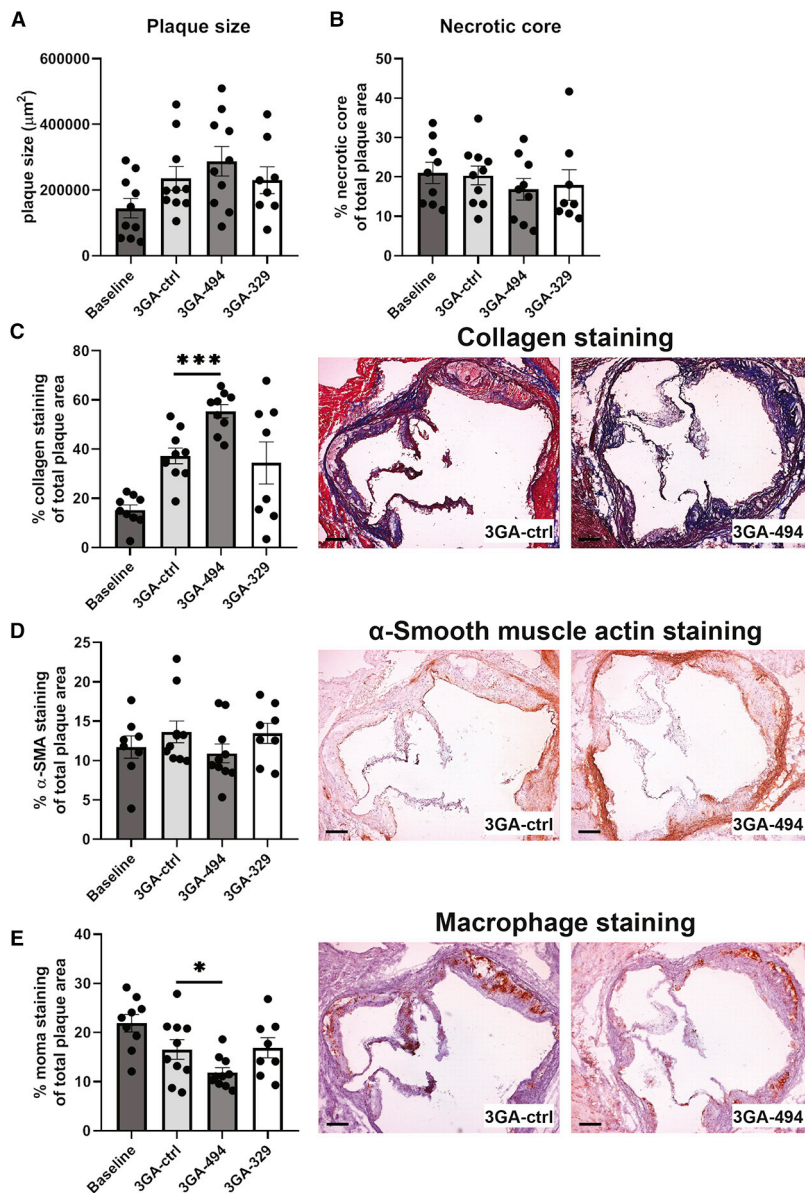
Figure 3. 3GA-494 Treatment Increased Plaque Stability in Aortic Root Plaques

(A) Plaque size in μm² of aortic root plaques, calculated from at least five 10-μm-thick sections of the three-valve area. (B) Necrotic core area, defined as an acellular area, measured in the lesions stained with Masson's trichrome; (C) collagen content, stained with Massons's trichrome; (D) SMC content, stained with an antibody against α-smooth muscle actin (α-SMA); and (E) macrophage content, stained with anti-monocyte-macrophage (Moma)-2 antibody. Amount of staining is shown as a percentage of total plaque area quantified in baseline (N = 10), 3GA-ctrl (N = 10), 3GA-494 (N = 10), and 3GA-329 (N = 8). (C–E) Scale bar, 250 μm. A two-tailed Student's t test was performed to compare single treatment to the 3GA-ctrl group. A Grubbs' test was used to identify significant outliers (α < 0.05). *p < 0.05, ***p < 0.0005 compared to 3GA-ctrl. Data are represented as mean ± SEM.

Splenic Megakaryocyte Retention

As mentioned above, all 3GA-494 mice and half of the 3GA-329 mice showed splenomegaly compared to 3GA-ctrl and baseline mice (Figures 5A and 5B). Staining for Von Willebrand factor (VWF) revealed strongly elevated numbers of megakaryocytes in the enlarged spleens of 3GA-494 mice compared to 3GA-ctrl, indicating increased megakaryopoiesis (Figures 5A and 5C). In 3GA-329 mice, only the mice with low platelet counts showed splenomegaly, accompanied by strongly elevated megakaryocyte numbers (Figure 5B). Despite the administration of a miRNA-494 inhibitor, splenic expression of miRNA-494 was upregulated 1 week after the final 3GA injection (Figure 5C). Increased expression of megakaryocyte/platelet markers, i.e., glycoprotein Ib platelet subunit alpha (GPIbα) and subunit beta (GpIbβ), both part of the platelet receptor complex for VWF, and integrin subunit beta 3 (Itgβ3), in the spleen of 3GA-494 mice confirmed indeed increased megakaryopoiesis (Figures 5D–5F). megakaryocytes and erythrocytes derive from a bipotent erythrocytic-megakaryocyte progenitor. Transcription factors involved in commitment of erythrocytic-megakaryocyte progenitor cells toward megakaryocyte progenitors and platelet production were also increased upon 3GA-494 treatment (Figures 5G–5I).[19] Expression of transcription factors involved in hematopoietic stem cell (HSC) proliferation and differentiation, which are putative targets of miRNA-494 and conserved in both human and mouse, as was predicted by http://www.targetscan.org (release 7.2), was similar in both 3GA-494- and 3GA-ctrl-treated mice (Figure S2C).[20–23] In the spleen of 3GA-329 mice, no significant differences in megakaryocyte/platelet markers or transcription factor expression was shown compared to 3GA-ctrl mice (Figures 5D–5I).

and, in particular, strongly reduced platelet count (Figures 4G and 4H). In the 3GA-329-treated mice, three mice showed reduced platelet counts, whereas platelet counts were normal in the remaining mice (Figure 4H).

Percentages of CD4+ and CD8+ T cells in the spleen were decreased in 3GA-494-treated mice and showed a trend toward a reduction in 3GA-329-treated mice (Figures S3F and S3G). However, since the spleens were enlarged due to proliferation of other cell types, as discussed below, the absolute numbers of CD4+ and CD8+ T cells may be similar among all groups. CD4+ and CD8+ T cells in the draining lymph nodes were not different among all groups (Figures S3H and S3I).

A previous study showed that in primary myelofibrosis, overexpression of miRNA-494 in HSCs promotes megakaryopoiesis via
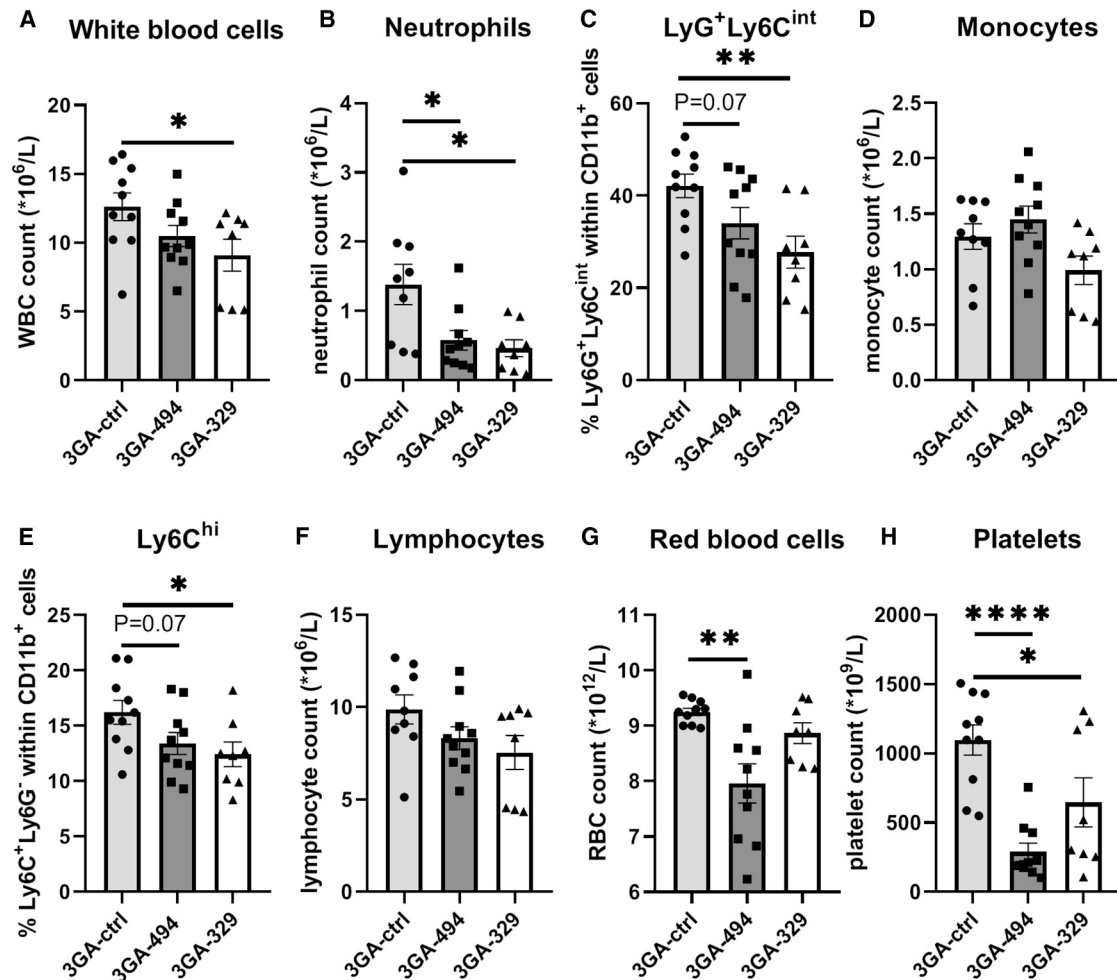
Figure 4. Blood Analysis of Mice Treated with 3GA-494, 3GA-329, or 3GA-ctrl 1 Week after Final Injection

(A–H) Amount of circulating (A) white blood cells (WBC; 10^6/L), (B) neutrophils (10^6/L), and (C) neutrophil marker lymphocyte antigen 6 complex, locus G6D (Ly6G$^+$) lymphocyte antigen 6 complex, locus C1 (Ly6C)^{int} cells defined as a percentage within CD11b$^+$ cells, (D) monocytes (10^6/L), and (E) inflammatory subset of monocyte Ly6G$^-$Ly6C^{hi} cells as a percentage within CD11b$^+$ cells, (F) lymphocytes (10^6/L), (G) red blood cells (RBC; 10^{12}/L), and (H) platelets (10^9/L). (A, C, and E–H) Blood cell analysis on whole blood quantified by Sysmex. (C and E) Fluorescence-activated cell sorting analysis (FACS) analysis performed on the blood of 3GA-ctrl, 3GA-494, and 3GA-329 mice after red blood cells were removed using lysis buffer. A two-tailed Student's t test was performed to compare single treatment to the 3GA-ctrl group. A Grubbs' test was used to identify significant outliers ($\alpha < 0.05$). *$p < 0.05$, **$p < 0.005$, ****$p < 0.0001$ compared to 3GA-ctrl. 3GA-ctrl (N = 10), 3GA-494 (N = 10), and 3GA-329 (N = 8). Data are represented as mean ± SEM.

downregulation of suppressor of cytokine signaling 6 (SOCS6).[24] We quantified SOCS6 expression in the spleen. However, SOCS6 expression showed a trend toward upregulation compared to 3GA-ctrl instead of downregulation (Figure S2D). As the bone marrow is also a source of megakaryopoiesis, we stimulated freshly isolated murine bone marrow cells with either 3GA-ctrl or 3GA-494. Although the miRNA-494 expression was downregulated in bone marrow cells after 3GA-494 treatment, we did not observe differences in SOCS6 expression nor in expression of transcription factors for megakaryocyte commitment and GPIbα and GpIbβ expression (Figures S2E and S2F).

Increased Hepatic Platelet Markers

Platelets can be cleared by hepatocytes and liver macrophages (Kuppfer cells).[25] Expression of miRNA-494 in the liver was similar in both 3GA-494 and 3GA-ctrl mice (Figure 6A). miRNA-329 was not expressed at all in the liver of either 3GA-329 or 3GA-ctrl mice (data not shown). Expression levels of platelet markers quantified by qPCR were upregulated in the liver of 3GA-494-treated mice, suggesting increased platelet clearance compared to 3GA-ctrl (Figures 6B–6D). In 3GA-329 mice, only the mice with low platelet counts showed increased expression of platelet markers in the liver (Figures 6B–6D).

Increased Expression of Platelet Receptors upon 3GA-494 Treatment

We further investigated whether 3GA-494 treatment could lead to miRNA-494 inhibition in anucleate platelets. Compared to 3GA-ctrl, mature miRNA-494 expression was first downregulated after
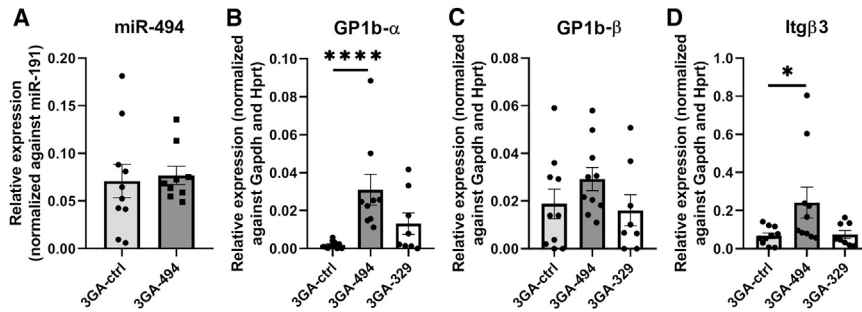
Figure 6. Increased Platelet Receptor Expression in the Liver of 3GA-494 Mice

(A) miRNA-494 expression in the liver of mice treated with 3GA-494 (N = 9) or 3GA-ctrl (N = 10), relative to miRNA-191. (B) Relative expression of three different platelet/megakaryocyte markers quantified by qPCR in the liver of 3GA-ctrl (N = 10), 3GA-494 (N = 10), and 3GA-329 (N = 8) mice; glycoprotein Ib platelet subunit alpha (GP1b-α), (C) beta chain (GP1b-β), and (D) integrin subunit beta 3 (Itgβ3) normalized to Gapdh and Hprt. (B–D) A Mann-Whitney U test was performed to compare single treatment to the 3GA-ctrl group. A Grubbs' test was used to identify significant outliers (α < 0.05). *p < 0.05, ****p < 0.0001, compared to 3GA-ctrl. Data are represented as mean ± SEM.

1 h and then upregulated after 4 h of incubation with 3GA-494 (Figure 7A). As platelets have no transcription, upregulation of miRNA-494 was accompanied by depletion of the primary miRNA-494 transcript, pri-miRNA-494, indicating rapid processing of the pri-miRNA-494 upon miRNA-494 downregulation (Figure 7B). Changes in the intermediate precursor miRNA-494, pre-miRNA-494, were less pronounced (Figure 7C).

Genes that we initially tested as housekeeping genes, including GAPDH, U6, and YWHAE, appeared to be unstable in 3GA-treated platelets (Figures S4B–S4D).[26] Pre-ITGβ3 showed stable expression and was, therefore, used as a housekeeping gene (Figure S4A). Pro-survival genes BCL2 and MCL1 are putative targets of miRNA-494, as was predicted by http://www.targetscan.org (release 7.2). Since miRNA-494 was upregulated in platelets, we checked whether BCL2 and MCL1 were downregulated, leading to more apoptosis and subsequently to more clearance. MCL1 appeared downregulated in 3GA-494, but BCL2 did not (Figures S4E and S4F).

Next, we quantified expression of platelet GPIBα and integrin subunit ITGβ3, both part of platelet receptors involved in platelet activation, and found upregulation after 4 h of 3GA-494 treatment compared to 3GA-ctrl (Figures 7D–7F). Since splicing occurs upon platelet activation, we measured pre-mRNA levels of MCL1, GAPDH, and GPIB-α.[27,28] Pre-mRNA levels were declined in 3GA-494-treated platelets compared to 3GA-ctrl, indicating increased splicing and hence increased platelet activation in 3GA-494-treated platelets (Figures S4G–S4I).

Time points from 8 h on were excluded, since all platelets, independent of their treatment, were hyper-activated in culture.

DISCUSSION

In this study, we first show that inhibition of 14q32 miRNAs, particularly miRNA-494, in mice with advanced atherosclerotic lesions halted carotid atherosclerotic plaque progression and promoted plaque stability in the aortic root of $LDLr^{-/-}$ mice. Second, plasma cholesterol levels were lowered further by 14q32 miRNA inhibition than by diet switch alone. Third, pro-atherogenic cells in the circulation, including pro-inflammatory monocytes (Ly6C^hi), neutrophils, and platelets were decreased after miRNA-329 and miRNA-494 inhibition.

Even though plasma cholesterol was lowered by diet switch, plaques in the carotid artery continued to grow in 3GA-ctrl mice. With 3GA-494 treatment and, in part, 3GA-329 treatment, we managed to halt plaque progression in the carotid artery. Although we combined 3GA treatment with plasma lipid lowering, plaque sizes from 3GA-494- and 3GA-329-treated mice were not significantly reduced compared to baseline, indicating that plaque regression did not occur in this setup. Unlike for the carotid artery lesions, neither 3GA-494 treatment nor 3GA-329 treatment resulted in reduced plaque sizes in the aortic root compared to 3GA-ctrl treatment. We have previously established that the expression of 14q32 miRNAs differs between sites of lesion development in mice,[14] and more recently, we demonstrated that expression of 14q32 miRNAs, including miRNA-494 and miRNA-329 and their targets, varies widely across the human vasculature as well.[29] Differences in response to miRNA inhibition in carotid artery plaques and aortic root plaques are, therefore, likely caused by differences in local miRNA and target gene expression. Although plaque size was not affected in the aortic root, plaque stability was clearly affected and increased after miRNA-494 inhibition, which is particularly relevant in reducing the risk of

---

Figure 5. Megakaryocyte Accumulation in the Spleen upon 3GA-494 and 3GA-329 Treatment

(A) Representative images of splenomegaly in 3GA-494-treated mice with megakaryocyte accumulation compared to 3GA-ctrl. Megakaryocytes were stained with an antibody against VWF. Scale bar, 500 μm. Zoomed-in image; scale bar, 50 μm. (B) Weight in g of the spleens of 3GA-ctrl (N = 10), 3GA-494 (N = 10), and 3GA-329 mice (N = 8). (C) Number of megakaryocytes per mm² spleen. (D) miRNA-494 expression in the spleen of 3GA-ctrl and 3GA-494 mice, relative to miRNA-191 expression. (E) Three different platelet/megakaryocyte markers quantified by qPCR in the spleen; glycoprotein Ib platelet subunit alpha (GP1b-α), (F) beta (GP1b-β) chain, and (G) integrin subunit beta 3 (Itgβ3) normalized to Gapdh and Hprt. (H–J) Transcription factors involved in megakaryocyte differentiation in the spleen. (H) Gata binding protein 1 (Gata1), (I) TAL bHLH transcription factor 1, erythroid differentiation factor (Tal1), and (J) nuclear factor, erythroid 2 (Nfe2). A two-tailed Student's t test was performed to compare single treatment to the 3GA-ctrl group. A Grubbs' test was used to identify significant outliers (α < 0.05). *p < 0.05, **p < 0.005, ****p < 0.0001 compared to 3GA-ctrl. 3GA-ctrl (N = 10), 3GA-494 (N = 10), and 3GA-329 (N = 8). Data are represented as mean ± SEM.
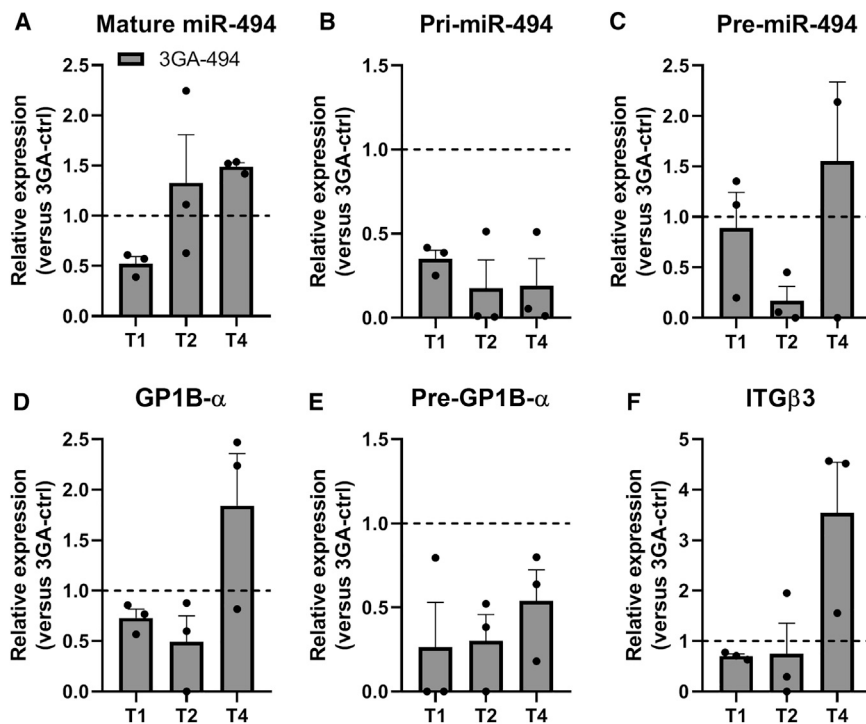
Figure 7. Upregulation of miRNA-494 Expression following 3GA-494 Treatment Led to Hyper-Activation of Platelets

Human platelets were incubated up to 4 h in PAS-III buffer with 30%–35% plasma with either 3GA-494 or 3GA-ctrl (in triplos). Platelets were kept in an incubator at 22°C with 5% CO_2 at continuously swirling. (A) Mature miRNA-494 expression, relative to miRNA-126. (B) Pri-miRNA-494 and (C) pre-miRNA-494 relative to pre-integrin subunit beta 3 (Itgβ3) expression. (D) Expression levels of platelet receptors glycoprotein Ib platelet subunit alpha (GP1B-α), (E) beta chain (GP1B-β), and (F) ITGβ3, relative to pre-ITGβ3 expression. All expression levels were normalized to 3GA-ctrl (100%). Data are represented as mean ± SEM.

cardiovascular events. These results indicate that 3GA-494 treatment would be relevant for treating different types of plaques, developing at different sites in the vasculature.

Collagen provides structural support in the fibrotic cap and in our study, particularly miRNA-494 inhibition increased intra-plaque collagen content in advanced lesions. Collagen is synthesized by SMCs, however, we have previously shown that miRNA-494 does not affect collagen synthesis.[14] Furthermore, even though miRNA-494 does affect proliferation of myofibroblasts,[15] neither miRNA-494 nor miRNA-329 inhibition affected the intra-plaque SMC content, which indicates that another mechanism caused the enhanced collagen deposition. We previously validated tissue inhibitor of metalloproteinases 3 (TIMP3) as a target of miRNA-494.[14] TIMP3 inhibits collagen degradation by matrix metalloproteinases (MMPs) and, therefore, more TIMP3 expression likely contributed to the observed increase in collagen content. Since macrophages produce MMPs, the reduced intra-plaque macrophage content may also have contributed to the increased collagen content in the plaques. Lipid-lowering strategies have been described to contribute to fewer intra-plaque macrophages.[30] Fewer intra-plaque macrophages are associated with a more stable plaque phenotype. In our study, macrophages in advanced plaques of 3GA-ctrl mice were decreased compared with baseline mice, which was likely an effect of plasma lipid lowering by diet switch, and additional treatment with 3GA-494 even further reduced intra-plaque macrophage numbers. Circulating inflammatory monocytes (Ly6C^{hi}) are associated with promoting plaque progression after extravasation into the lesion

and here, both miRNA-494 and miRNA-329 inhibition resulted in a reduction in circulating pro-inflammatory Ly6C^{hi} monocytes, which may have caused the reduction in plaque macrophages. In addition, platelets have been described to mediate monocyte activation, recruitment, and extravasation into the lesion.[31] Therefore, the strongly reduced blood platelet levels in 3GA-494 mice may also have contributed to a reduction in macrophage extravasation into the lesion.

Particularly, 3GA-494 mice showed reduced levels of circulating inflammatory cells, including neutrophils, red blood cells, and platelets, all of which originate from a common early-myeloid progenitor cell. Decreased expression of miRNA-494 has been reported to drive chronic myeloid leukemia, a stem-cell-derived malignant disorder in human.[32] We measured whether transcription factors involved in HSC proliferation and differentiation were targeted by increased miRNA-494 expression in the spleen. However, expression levels were not affected, indicating that this was not primary cause of reduced levels of circulating neutrophils, red blood cells, and platelets in 3GA-494 mice. Others have also described a role for 14q32 miRNAs, including miRNA-494, in human erythropoiesis and, therefore, proper development of erythrocytes in our murine model may have been targeted by 3GA-494 treatment.[33] Exact mechanisms on how myeloid cells in the circulation are reduced, however, remains to be determined in future research.

In previous studies, we have shown that multiple miRNAs transcribed from the 14q32 cluster are involved in different processes of vascular remodeling.[14–17] Inhibition of 14q32 miRNAs miRNA-494, miRNA-329, miRNA-487b, and miRNA-495 improved neovascularization and blood flow recovery in a hindlimb ischemia model.[15] Neovascularization requires a pro-inflammatory response, whereas an anti-inflammatory response is favorable for atherosclerosis. Stimulation of neovascularization often leads to aggravation of atherosclerosis and vice versa.[34] This effect is often referred to as the Janus phenomenon,

after the two-faced Roman god.[35] In contrast to the Janus phenomenon, 14q32 miRNA inhibition both increases neovascularization and reduces atherosclerosis and, therefore, plays a unique role in vascular remodeling.

Strongly increased megakaryocyte content and increased expression of transcription factors in the spleen of 3GA-494 mice clearly showed increased commitment toward the megakaryocyte lineage. Since SOCS6 expression was not affected upon 3GA-494 treatment in either the spleen or bone marrow cells, this indicates that megakaryocyte differentiation was not targeted by 3GA-494 treatment. Increased splenic megakaryocyte differentiation in 3GA-494 mice is, therefore, likely a compensatory mechanism to prevent severe thrombocytopenia. Others have also demonstrated that mice show increased megakaryocyte differentiation as a response to lower platelet counts.[36]

The underlying mechanism of platelet exhaustion may be an increased hepatic clearance. We found increased platelet receptor expression in the liver. Apoptotic platelets are recognized and cleared by the liver.[37] However, pro-survival genes Mcl-1 and Bcl-2 were not clearly affected by miRNA-494 expression in the platelets and were therefore unlikely the key contributors to increased platelet clearance. Activation of the platelet receptor GPIb-IX can also lead to rapid hepatic clearance, and differential expression of the 14q32 cluster has previously been linked to platelet reactivity.[37–39] Indeed, we found that upregulation of miRNA-494 expression following 3GA-494 treatment led to hyper-activation of platelets. Also, as miRNA-494 expression in the liver itself was not affected by 3GA-494, it is most likely that increased platelet clearance is caused by platelet activation in response to 3GA-494 treatment, rather than by upregulation of clearance pathways in the liver.

A surprising observation in this study is the fact that in both platelets and in the spleen, 3GA-494 treatment resulted in short-term miRNA-494 inhibition followed by a clear miRNA-494 upregulation. The upregulation was accompanied by rapid depletion of miRNA-494 precursors in platelets. RNA binding proteins, which are regulated by miRNAs themselves, are able to regulate miRNA processing in a cell-specific manner. In a previous study, we have demonstrated post-transcriptional regulation of miRNA-494 by Mef2A, which directly binds to pri-miRNA-494.[17] However, which precise mechanism underlies the cell- and tissue-specific autoregulation of miRNA-494 in $LDLr^{-/-}$ mice remains to be determined.

Since each cell type has its own specific miRNA and target gene expression pattern, single miRNA inhibition has distinct effects in each cell type.[29,40,41] Above, we have discussed the effects of miRNA-494 and miRNA-329 inhibition on SMCs and myofibroblasts, on macrophages, and on megakaryocyte cells and platelets, but also the endothelial cell is of importance in atherosclerosis development and progression. We have shown in the past that inhibition of miRNA-494 had little effect on proliferation of human arterial endothelial cells. Inhibition of miRNA-329, however, increased proliferation of endothelial cells.[15] Whether inhibition of miRNA-329 affects

plaque size and composition via increased proliferation of endothelial cells remains for future research.

In our study, we used a scrambled 3GA as control, and in a previous study we have established that this 3GA-ctrl does not show significant differences as compared to vehicle controls.[15] Non-specific effects of this 3GA-ctrl in this study are thus highly unlikely; however, they cannot be completely excluded. In addition, in this study, we used $LDLr^{-/-}$, which is a strain that allows plasma lipid lowering in response to a diet switch. Previously, we have shown therapeutic effects of 3GA-494 in an $ApoE^{-/-}$ mouse model, in which atherosclerosis develops in response to elevated lipid levels, which cannot be lowered using a diet switch. The data from these two studies may thus not be directly comparable due to strain differences; however, in both models, 3GA-494 treatment improved lesion size and stability. The most important strength of this study is that we used a murine model with fully established lesions and started 3GA treatment after advanced plaques had been formed, while most studies focus on initial lesion development. Additionally, we included a lipid-lowering strategy by changing the diet from high-fat high-cholesterol to regular chow. Since most patients present in the clinic with advanced and unstable atherosclerosis and receive routine lipid-lowering treatment, we more closely mimicked the clinical situation in this study.

Conclusions

In conclusion, inhibition of 14q32 miRNAs, and particularly of miRNA-494, halts plaque progression and increases plaque stability in mice with established advanced atherosclerotic lesions. Plasma cholesterol levels were lowered further by 14q32 miRNA inhibition than by diet switch alone. Furthermore, pro-atherogenic cells, including inflammatory Ly6C^{hi} monocytes, neutrophils, and platelets, were reduced in the circulation. Inhibition of miRNA-494 would therefore be a potential therapeutic target for stabilizing vulnerable lesions in patients and may even prevent surgical interventions in some cases.

MATERIALS AND METHODS

Mice and Experimental Design

All animal work performed conforms to the guidelines from the Dutch government and the Directive 2010/63/EU of the European Parliament, and all experiments were approved by the local animal ethics committee (DEC number 14103). Male $LDLr^{-/-}$ mice, aged 8 to 9 weeks, were obtained from our in-house breeding facility (Gorlaeus Laboratories, Leiden University, Leiden, the Netherlands). Food and water were available *ad libitum*.

The timeline of the study is shown in Figure S1. All mice were fed a Western-type diet (WTD) containing 0.25% cholesterol and 15% cacao butter (SDS, Sussex, UK) for 10 weeks to induce advanced atherosclerotic lesions, as described previously.[42] Four weeks after start of the WTD, mice underwent surgical interventions in order to induce carotid artery plaque formation. As described previously, semi-constrictive collars were placed around both carotid arteries.[14] Mice were anaesthetized by subcutaneous injection of ketamine

(60 mg/kg; Eurovet Animal Health, Bladel, the Netherlands), fentanyl citrate, and fluanisone (1.26 mg/kg and 2 mg/kg, respectively; Janssen Animal Health, Sauderton, UK).

Six weeks after collar placement, mice were age-, cholesterol-, and weight-matched to ensure an equal distribution over all groups before start of the treatment. At that time point, a subset of mice (n = 10) was sacrificed as baseline control. The remaining mice were placed on a regular chow diet to lower plasma cholesterol levels, and 3GAs against miRNA-494 (3GA-494; n = 10), miRNA-329 (3GA-329; n = 10), or negative control (3GA-ctrl; n = 10) was administered via the tail vein (intravenously [i.v.]) at a concentration of 1 mg/mouse. 3GAs were designed with perfect reverse complementary to the mature target miRNA sequence and synthesized by Idera Pharmaceuticals (Cambridge, MA, USA). The same sequences of 3GAs (formerly named gene-silencing oligonucleotides [GSOs]) against miRNA-494 and miRNA-329 were used as described previously.[15] As a negative control, a scrambled sequence was used, designed not to target any known murine miRNA. Sequences of the miRNAs and 3GAs are shown in Table S1. Second and third injections were given 2 and 4 weeks after diet switch. During the experiment, total serum cholesterol levels were quantified by enzymatic procedures using Precipath (Roche Diagnostics, Mannheim, Germany). One week after the final 3GA injection, mice were anaesthetized by a subcutaneous injection of a cocktail containing ketamine (40 mg/mL), atropine (50 μg/mL), and sedazine (6.25 mg/mL). Mice were subsequently perfused with PBS through the left cardiac ventricle, after which carotid arteries and other organs were collected, frozen, and used for further analysis. At sacrifice, whole blood was analyzed on a Sysmex XT-2000i analyzer (Goffin Meyvis, Etten Leur, the Netherlands).

Flow Cytometric Analysis
At sacrifice, blood, spleen, and the mediastinal lymph nodes near the heart (HLN) were isolated. Single-cell suspensions of spleen and HLN were obtained by squeezing the organs through a 70-μm cell strainer. Red blood cells were removed using Ammonium-Chloride-Potassium (ACK) lysis buffer (0.15 M NH_4Cl, 10 mM $NaHCO_3$, 0.1 mM EDTA [pH 7.3]). Immune cells were analyzed with flow cytometry: T cells ($CD4^+$, $CD8^+$), B cells ($CD19^+$), neutrophils ($CD11b^+Ly6G^+$), and inflammatory monocytes ($CD11b^+Ly6G^-Ly6C^{high}$). FACS analysis was performed on a FACSCantoII (BD Biosciences), and data was analyzed with FlowJo software (Treestar).

RNA Isolation and qRT-PCR
Frozen tissues were crushed by use of pestle and mortar while immersed in liquid nitrogen. After homogenizing and complete evaporation of the liquid nitrogen, TRIzol (Thermo Fisher, Bleiswijk, the Netherlands) was added to the samples. For carotid artery RNA isolation, carotid artery segments from three to four mice were pooled and homogenized with a pellet crusher in TRIzol. Total RNA was isolated by standard TRIzol-chloroform extraction. RNA concentration and purity were measured on the Nanodrop (Nanodrop Technologies).

For miRNAs, miRNA-specific Taqman qPCR kits (Thermo Fisher, Bleiswijk, the Netherlands) were used for reversed transcription and quantification by qPCR according to the manufacturers protocol. For mRNA, RNA was reverse transcribed using a "high-capacity RNA to cDNA" kit (Thermo Fisher, Bleiswijk, the Netherlands). SybrGreen reagents (QIAGEN Benelux, Venlo, the Netherlands) were used for the qPCR. The data were normalized using a stably expressed endogenous control. miRNA-191 was used for miRNAs and Gapdh and Hprt for mRNA. qPCR was performed on the VIIa7 (Applied Biosystems).

Immunohistochemistry
Frozen sections of carotid arteries (10 μm thick) were fixed with Formal-Fixx (Thermo Fisher, Bleiswijk, the Netherlands) for 30 min and subsequently stained with H&E to determine plaque size. Analysis was performed on sections throughout the atherosclerotic lesion (100 μm apart, resulting in the average plaque size value) and at the site of maximal stenosis, the site/section of the plaque that has the largest plaque size, using Leica Qwin software, as described previously.[43] Mice with plaques containing a reorganized thrombus were excluded from the plaque size analysis (three mice in baseline, four mice in 3GA-ctrl, one mouse in 3GA-494, and one mouse in 3GA-329).

To determine lesion size in the three-valve area, cryosections (10 μm thick) of the aortic root were stained with oil red O and hematoxylin (Sigma-Aldrich, Zwijndrecht, the Netherlands). Lesion size was calculated from at least five 10-μm-thick sections of the three-valve area. Masson's trichrome staining was used to visualize collagen and determine necrotic core area. Plaque macrophages were stained using a MOMA-2 antibody at a 1:1,000 concentration (rat IgG2b, Serotec, Kidlington, UK). SMCs were stained with α-smooth muscle actin antibody (Clone 1A4, 1:1,000, Abcam, Cambridge, UK). Neutrophils were stained using the Naphthol AS-D chloroacetate kit (Sigma-Aldrich, Zwijndrecht, the Netherlands). Collagen, necrotic core size, SMCs, macrophages, and neutrophils were defined as percentage of total plaque area using Leica Qwin software.

Frozen cross-sections of spleen and liver were prepared (6 μm thickness) and fixed in ice-cold acetone. An antibody against VWF (A0082, 1:1000, Dako, Santa Clara, CA, USA) was used to visualize megakaryocytes in the spleen. Megakaryocytes were counted manually. ImageJ software was used for area measurements.

Bone Marrow Cells
To isolate bone marrow (BM) cells, femurs and tibias of C57BL/6 mice were dissected, and the bone marrow was flushed with PBS. BM cells were filtered through a 70-μm cell strainer, centrifuged at 300 × g for 15 min, and suspended in RPMI 1640 medium containing L-glutamine supplemented with 10% heat-inactivated fetal calf serum (FCSi) and 1% penicillin/streptomycin (P/S). BM cells were plated at a concentration of 1.8×10^6 cells/mL and stimulated with 3GA-494 or 3GA-ctrl at a concentration of 10 ng/μL for 48 h

in an incubator at 37°C with 5% CO_2. After 48 h of incubation, cells were washed with PBS and resuspended in TRIzol for subsequent RNA isolations.

Human Platelets

Platelets, pooled from five different healthy donors with blood type O and Rh positive, were obtained from a blood bank facility (Sanquin, Amsterdam, the Netherlands). The same conditions as used for storage in platelet transfusion were used in the experiment. Platelets in PAS-III buffer with 30%–35% plasma were transferred from the transfusion bag into 6-well plates and kept in an incubator at 22°C with 5% CO_2 at continuously swirling. Platelet concentration was 0.9–1.3×10^9/mL and contained $< 1 \times 10^6$ leukocytes. Platelets were untreated, or 3GA-494 or 3GA-ctrl was added at a concentration of 10 ng/μL and incubated for up to 48 h. As a quality control, pH was measured at each time point, and platelet parameters were measured by Sysmex. To pellet the platelets after treatments, platelets were centrifuged at $800 \times g$ for 15 min at room temperature and subsequently resuspended in TRIzol.

Statistical Analyses

Results are expressed as mean ± SEM. A Kolmogorov-Smirnov test was performed to check normal distribution of values. When values were normally distributed, a two-tailed Student's t test was used to compare single-treatment group with the control group. When values were not normally distributed, a Mann-Whitney U test was performed to compare single treatment with the control group. $p < 0.05$ was considered significant. A Grubbs' test was used to identify significant outliers (α < 0.05).

SUPPLEMENTAL INFORMATION

Supplemental Information can be found online at https://doi.org/10.1016/j.omtn.2019.09.021.

AUTHOR CONTRIBUTIONS

E.v.I., A.C.F., I.B., and A.Y.N. designed the experiments; E.v.I., A.C.F., M.J.K, I.B., and A.Y.N. conducted the experiments; E.v.I., A.C.F., I.B., A.Y.N., J.K., and P.H.A.Q. wrote, reviewed, and edited the paper; I.B. and A.Y.N. acquired funding; I.B., A.Y.N., and P.H.A.Q. supervised.

CONFLICTS OF INTEREST

The authors declare no competing interests.

ACKNOWLEDGMENTS

REFERENCES

1. Libby, P., Ridker, P.M., and Hansson, G.K. (2011). Progress and challenges in translating the biology of atherosclerosis. Nature 473, 317–325.

2. Bonati, L.H., Dobson, J., Featherstone, R.L., Ederle, J., van der Worp, H.B., de Borst, G.J., Mali, W.P., Beard, J.D., Cleveland, T., Engelter, S.T., et al.; International Carotid Stenting Study investigators (2015). Long-term outcomes after stenting versus endarterectomy for treatment of symptomatic carotid stenosis: the International Carotid Stenting Study (ICSS) randomised trial. Lancet 385, 529–538.

3. Stone, N.J., Robinson, J.G., Lichtenstein, A.H., Bairey Merz, C.N., Blum, C.B., Eckel, R.H., Goldberg, A.C., Gordon, D., Levy, D., Lloyd-Jones, D.M., et al.; American College of Cardiology/American Heart Association Task Force on Practice Guidelines (2014). 2013 ACC/AHA guideline on the treatment of blood cholesterol to reduce atherosclerotic cardiovascular risk in adults: a report of the American College of Cardiology/American Heart Association Task Force on Practice Guidelines. Circulation 129 (Suppl 2), S1–S45.

4. Steen, D.L., Khan, I., Ansell, D., Sanchez, R.J., and Ray, K.K. (2017). Retrospective examination of lipid-lowering treatment patterns in a real-world high-risk cohort in the UK in 2014: comparison with the National Institute for Health and Care Excellence (NICE) 2014 lipid modification guidelines. BMJ Open 7, e013255.

5. Crisby, M., Nordin-Fredriksson, G., Shah, P.K., Yano, J., Zhu, J., and Nilsson, J. (2001). Pravastatin treatment increases collagen content and decreases lipid content, inflammation, metalloproteinases, and cell death in human carotid plaques: implications for plaque stabilization. Circulation 103, 926–933.

6. Ridker, P.M., Everett, B.M., Thuren, T., MacFadyen, J.G., Chang, W.H., Ballantyne, C., Fonseca, F., Nicolau, J., Koenig, W., Anker, S.D., et al.; CANTOS Trial Group (2017). Antiinflammatory Therapy with Canakinumab for Atherosclerotic Disease. N. Engl. J. Med. 377, 1119–1131.

7. Welten, S.M., Goossens, E.A., Quax, P.H., and Nossent, A.Y. (2016). The multifactorial nature of microRNAs in vascular remodelling. Cardiovasc. Res. 110, 6–22.

8. Najafi-Shoushtari, S.H., Kristo, F., Li, Y., Shioda, T., Cohen, D.E., Gerszten, R.E., and Näär, A.M. (2010). MicroRNA-33 and the SREBP host genes cooperate to control cholesterol homeostasis. Science 328, 1566–1569.

9. Rayner, K.J., Sheedy, F.J., Esau, C.C., Hussain, F.N., Temel, R.E., Parathath, S., van Gils, J.M., Rayner, A.J., Chang, A.N., Suarez, Y., et al. (2011). Antagonism of miR-33 in mice promotes reverse cholesterol transport and regression of atherosclerosis. J. Clin. Invest. 121, 2921–2931.

10. Rayner, K.J., Suárez, Y., Dávalos, A., Parathath, S., Fitzgerald, M.L., Tamehiro, N., Fisher, E.A., Moore, K.J., and Fernández-Hernando, C. (2010). MiR-33 contributes to the regulation of cholesterol homeostasis. Science 328, 1570–1573.

11. Price, N.L., Rotllan, N., Canfrán-Duque, A., Zhang, X., Pati, P., Arias, N., Moen, J., Mayr, M., Ford, D.A., Baldán, Á., et al. (2017). Genetic Dissection of the Impact of miR-33a and miR-33b during the Progression of Atherosclerosis. Cell Rep. 21, 1317–1330.

12. Nazari-Jahantigh, M., Wei, Y., Noels, H., Akhtar, S., Zhou, Z., Koenen, R.R., Heyll, K., Gremse, F., Kiessling, F., Grommes, J., et al. (2012). MicroRNA-155 promotes atherosclerosis by repressing Bcl6 in macrophages. J. Clin. Invest. 122, 4190–4202.

13. Eken, S.M., Jin, H., Chernogubova, E., Li, Y., Simon, N., Sun, C., Korzunowicz, G., Busch, A., Bäcklund, A., Österholm, C., et al. (2017). MicroRNA-210 Enhances Fibrous Cap Stability in Advanced Atherosclerotic Lesions. Circ. Res. 120, 633–644.

14. Wezel, A., Welten, S.M., Razawy, W., Lagraauw, H.M., de Vries, M.R., Goossens, E.A., Boonstra, M.C., Hamming, J.F., Kandimalla, E.R., Kuiper, J., et al. (2015). Inhibition of MicroRNA-494 Reduces Carotid Artery Atherosclerotic Lesion Development and Increases Plaque Stability. Ann. Surg. 262, 841–847, discussion 847–848.

15. Welten, S.M., Bastiaansen, A.J., de Jong, R.C., de Vries, M.R., Peters, E.A., Boonstra, M.C., Sheikh, S.P., La Monica, N., Kandimalla, E.R., Quax, P.H., and Nossent, A.Y. (2014). Inhibition of 14q32 MicroRNAs miR-329, miR-487b, miR-494, and miR-495 increases neovascularization and blood flow recovery after ischemia. Circ. Res. 115, 696–708.

16. Welten, S.M.J., de Jong, R.C.M., Wezel, A., de Vries, M.R., Boonstra, M.C., Parma, L., Jukema, J.W., van der Sluis, T.C., Arens, R., Bot, I., et al. (2017). Inhibition of 14q32 microRNA miR-495 reduces lesion formation, intimal hyperplasia and plasma cholesterol levels in experimental restenosis. Atherosclerosis 261, 26–36.

17. Welten, S.M.J., de Vries, M.R., Peters, E.A.B., Agrawal, S., Quax, P.H.A., and Nossent, A.Y. (2017). Inhibition of Mef2a Enhances Neovascularization via Post-transcriptional Regulation of 14q32 MicroRNAs miR-329 and miR-494. Mol. Ther. Nucleic Acids 7, 61–70.

18. Foks, A.C., van Puijvelde, G.H., Bot, I., ter Borg, M.N., Habets, K.L., Johnson, J.L., Yagita, H., van Berkel, T.J., and Kuiper, J. (2013). Interruption of the OX40-OX40 ligand pathway in LDL receptor-deficient mice causes regression of atherosclerosis. J. Immunol 191, 4573–4580.

19. Fuhrken, P.G., Chen, C., Apostolidis, P.A., Wang, M., Miller, W.M., and Papoutsakis, E.T. (2008). Gene Ontology-driven transcriptional analysis of CD34+ cell-initiated megakaryocytic cultures identifies new transcriptional regulators of megakaryopoiesis. Physiol. Genomics 33, 159–169.

20. Magnusson, M., Brun, A.C., Miyake, N., Larsson, J., Ehinger, M., Bjornsson, J.M., Wutz, A., Sigvardsson, M., and Karlsson, S. (2007). HOXA10 is a critical regulator for hematopoietic stem cells and erythroid/megakaryocyte development. Blood 109, 3687–3696.

21. Tanabe, O., Shen, Y., Liu, Q., Campbell, A.D., Kuroha, T., Yamamoto, M., and Engel, J.D. (2007). The TR2 and TR4 orphan nuclear receptors repress Gata1 transcription. Genes Dev. 21, 2832–2844.

22. Chen, Z., Yi, W., Morita, Y., Wang, H., Cong, Y., Liu, J.P., Xiao, Z., Rudolph, K.L., Cheng, T., and Ju, Z. (2015). Wip1 deficiency impairs haematopoietic stem cell function via p53 and mTORC1 pathways. Nat. Commun. 6, 6808.

23. Nemeth, M.J., Kirby, M.R., and Bodine, D.M. (2006). Hmgb3 regulates the balance between hematopoietic stem cell self-renewal and differentiation. Proc. Natl. Acad. Sci. USA 103, 13783–13788.

24. Rontauroli, S., Norfo, R., Pennucci, V., Zini, R., Ruberti, S., Bianchi, E., Salati, S., Prudente, Z., Rossi, C., Rosti, V., et al. (2017). miR-494-3p overexpression promotes megakaryocytopoiesis in primary myelofibrosis hematopoietic stem/progenitor cells by targeting SOCS6. Oncotarget 8, 21380–21397.

25. Sørensen, A.L., Rumjantseva, V., Nayeb-Hashemi, S., Clausen, H., Hartwig, J.H., Wandall, H.H., and Hoffmeister, K.M. (2009). Role of sialic acid for platelet life span: exposure of beta-galactose results in the rapid clearance of platelets from the circulation by asialoglycoprotein receptor-expressing liver macrophages and hepatocytes. Blood 114, 1645–1654.

26. Mossberg, K., Svensson, P.A., Gidlöf, O., Erlinge, D., Jern, S., and Brogren, H. (2016). Normalization of qPCR in platelets - YWHAE a potential genericreference gene. Platelets 27, 729–734.

27. Denis, M.M., Tolley, N.D., Bunting, M., Schwertz, H., Jiang, H., Lindemann, S., Yost, C.C., Rubner, F.J., Albertine, K.H., Swoboda, K.J., et al. (2005). Escaping the nuclear confines: signal-dependent pre-mRNA splicing in anucleate platelets. Cell 122, 379–391.

28. Nassa, G., Giurato, G., Cimmino, G., Rizzo, F., Ravo, M., Salvati, A., Nyman, T.A., Zhu, Y., Vesterlund, M., Lehtiö, J., et al. (2018). Splicing of platelet resident pre-mRNAs upon activation by physiological stimuli results in functionally relevant proteome modifications. Sci. Rep. 8, 498.

29. Goossens, E.A.C., de Vries, M.R., Simons, K.H., Putter, H., Quax, P.H.A., and Nossent, A.Y. (2019). miRMap: Profiling 14q32 microRNA Expression and DNA Methylation Throughout the Human Vasculature. Front. Cardiovasc. Med 6, 113.

30. Feig, J.E., Parathath, S., Rong, J.X., Mick, S.L., Vengrenyuk, Y., Grauer, L., Young, S.G., and Fisher, E.A. (2011). Reversal of hyperlipidemia with a genetic switch favor-ably affects the content and inflammatory state of macrophages in atherosclerotic plaques. Circulation 123, 989–998.

31. Badrnya, S., Schrottmaier, W.C., Kral, J.B., Yaiw, K.C., Volf, I., Schabbauer, G., Söderberg-Nauclér, C., and Assinger, A. (2014). Platelets mediate oxidized low-density lipoprotein-induced monocyte extravasation and foam cell formation. Arterioscler. Thromb. Vasc. Biol. 34, 571–580.

32. Salati, S., Salvestrini, V., Carretta, C., Genovese, E., Rontauroli, S., Zini, R., Rossi, C., Ruberti, S., Bianchi, E., Barbieri, G., et al. (2017). Deregulated expression of miR-29a-3p, miR-494-3p and miR-660-5p affects sensitivity to tyrosine kinase inhibitors in CML leukemic stem cells. Oncotarget 8, 49451–49469.

33. Lessard, S., Beaudoin, M., Orkin, S.H., Bauer, D.E., and Lettre, G. (2018). 14q32 and let-7 microRNAs regulate transcriptional networks in fetal and adult human erythroblasts. Hum. Mol. Genet. 27, 1411–1420.

34. Parma, L., Baganha, F., Quax, P.H.A., and de Vries, M.R. (2017). Plaque angiogenesis and intraplaque hemorrhage in atherosclerosis. Eur. J. Pharmacol. 816, 107–115.

35. Epstein, S.E., Stabile, E., Kinnaird, T., Lee, C.W., Clavijo, L., and Burnett, M.S. (2004). Janus phenomenon: the interrelated tradeoffs inherent in therapies designed to enhance collateral formation and those designed to inhibit atherogenesis. Circulation 109, 2826–2831.

36. Barwari, T., Eminaga, S., Mayr, U., Lu, R., Armstrong, P.C., Chan, M.V., Sahraei, M., Fernández-Fuertes, M., Moreau, T., Barallobre-Barreiro, J., et al. (2018). Inhibition of profibrotic microRNA-21 affects platelets and their releasate. JCI Insight 3, 123335.

37. Quach, M.E., Chen, W., and Li, R. (2018). Mechanisms of platelet clearance and translation to improve platelet storage. Blood 131, 1512–1521.

38. Deng, W., Xu, Y., Chen, W., Paul, D.S., Syed, A.K., Dragovich, M.A., Liang, X., Zakas, P., Berndt, M.C., Di Paola, J., et al. (2016). Platelet clearance via shear-induced unfolding of a membrane mechanoreceptor. Nat. Commun. 7, 12863.

39. Edelstein, L.C., Simon, L.M., Montoya, R.T., Holinstat, M., Chen, E.S., Bergeron, A., Kong, X., Nagalla, S., Mohandas, N., Cohen, D.E., et al. (2013). Racial differences in human platelet PAR4 reactivity reflect expression of PCTP and miR-376c. Nat. Med. 19, 1609–1616.

40. Santulli, G. (2015). microRNAs Distinctively Regulate Vascular Smooth Muscle and Endothelial Cells: Functional Implications in Angiogenesis, Atherosclerosis, and In-Stent Restenosis. Adv. Exp. Med. Biol. 887, 53–77.

41. Rogg, E.M., Abplanalp, W.T., Bischof, C., John, D., Schulz, M.H., Krishnan, J., Fischer, A., Poluzzi, C., Schaefer, L., Bonauer, A., et al. (2018). Analysis of Cell Type-Specific Effects of MicroRNA-92a Provides Novel Insights Into Target Regulation and Mechanism of Action. Circulation 138, 2545–2558.

42. van Duijn, J., Kritikou, E., Benne, N., van der Heijden, T., van Puijvelde, G.H., Kröner, M.J., Schaftenaar, F.H., Foks, A.C., Wezel, A., Smeets, H., et al. (2019). CD8+ T-cells contribute to lesion stabilization in advanced atherosclerosis by limiting macrophage content and CD4+ T-cell responses. Cardiovasc. Res. 115, 729–738.

43. Bot, I., Ortiz Zacarías, N.V., de Witte, W.E., de Vries, H., van Santbrink, P.J., van der Velden, D., Kröner, M.J., van den Berg, D.J., Stamos, D., de Lange, E.C., et al. (2017). A novel CCR2 antagonist inhibits atherogenesis in apoE deficient mice by achieving high receptor occupancy. Sci. Rep. 7, 52.